

Nonlinear Stability of Plane Wave Solutions of the Nonlocal Nonlinear Schrödinger Equation

Brandon G. Bale, Bernard Deconinck, and J. Nathan Kutz
Department of Applied Mathematics
University of Washington
Seattle, WA 98195, USA

April 26, 2007

Abstract

The nonlinear stability of plane wave solutions of the nonlocal nonlinear Schrödinger equation (NNLS) is examined. For Bose-Einstein condensates (BECs), the nonlocality is a consequence of an interatomic interaction potential. The same nonlocality arises in nonlinear optics due to an electric time response of the material to an external electric field. In the model we consider, we do not resort to the standard delta function approximation giving rise to the nonlinear Schrödinger equation (NLS). The nature of the instabilities is characterized by the Fourier transform of the nonlocal kernel and the amplitude of the plane wave solution. Conditions are found determining the nonlinear stability of plane waves. Including the nonlocality gives a more meaningful description of microscopic interactions which has a profound effect on the dynamics. If the typical width of the nonlocal kernel is small, a moment expansion is often used to obtain a local approximation. We discuss the limited validity of this approximation and show how the stability of the approximated equation differs from that of the nonlocal equation.

1 Introduction

In all applications where the nonlinear Schrödinger (NLS) equation is relevant, it arises as a simplified model of a nonlocal governing equation. In two applications, Bose-Einstein condensates [1, 2] and nonlinear optics [3], the same nonlinear nonlocal equation

$$i\psi_t = -\frac{1}{2}\nabla^2\psi + \alpha\psi \int_{-\infty}^{\infty} R(\mathbf{r} - \mathbf{r}') |\psi(\mathbf{r}', t)|^2 d\mathbf{r}' \quad (1)$$

governs the dynamics under fairly general circumstances. For a Bose-Einstein condensate (BEC), we consider the dynamics of N identical pairwise interacting particles governed by the Schrödinger

equation [4]. To arrive at a mean-field description of the ground state, one can apply Lagrangian reduction [5] and the Hartree approximation. An additional zero temperature limit leads to Eq. (1) [1, 2]. The governing equation (1) describes the ground-state wave function ψ . Since our primary focus here is on the dynamics associated with the nonlocality, we exclude any external potential and focus on the interaction potential $R(\mathbf{r})$. This is different from [7], where the stability of periodic solutions of Eq. (1) with an external periodic potential was considered, leading to a singular instability. The parameter $\alpha = \pm 1$ determines whether the interaction potential is repulsive or attractive. We normalize R such that $\int_{-\infty}^{\infty} R(\mathbf{r}) d\mathbf{r} = 1$ and $R(\mathbf{0}) > 0$. In most cases $R(\mathbf{r})$ is a short-range interaction potential, and is often approximated by a Dirac delta function $\delta(\mathbf{r})$, giving the Nonlinear Schrödinger equation [1, 2]

$$i\psi_t = -\frac{1}{2}\nabla^2\psi + \alpha|\psi|^2\psi. \quad (2)$$

However, this approximation is not consistent with the mean-field approximations made earlier which rely on the dilute nature of the BEC. Both Eq. (1) and Eq. (2) are formal asymptotic descriptions of a BEC. Note that Lieb and Seiringer [6], following a different derivation, proved rigorously that the stationary Gross-Pitaevskii equation does indeed describe the ground state of the BEC.

In nonlinear optics, the response of a particular medium to an applied electric field generates an assortment of nonlinear phenomena [8]. These phenomena are the result of an induced polarization in Maxwell's equations. To describe the induced polarization, we assume the nonlinear polarization density interacts with the macroscopic electric field locally in space and through the electric dipole interaction. In media whose electronic gap frequency is much higher than any optical frequencies present, the electrons follow nearly adiabatically both the external electric field and the fluctuating fields of the nuclei. Using the adiabatic approximation, the presence of the electrons is manifested as an effective nonlinear potential in the nuclear Hamiltonian [8]. For materials that are isotropic and have inversion symmetry, the induced polarization is described by linear and cubic nonlocal terms. Expanding the linear nonlocality around some time t and shifting to moving coordinates, we obtain the governing equation (1) where ψ is the envelope of the electric field $E(\mathbf{r}, t) = \psi(\mathbf{r}, t)e^{i(\mathbf{k}\cdot\mathbf{r}-\omega t)} + \text{c.c.}$ Here $R(\mathbf{r})$ is a one-sided time response of the medium (electrons) to the electric field. The parameter $\alpha = \pm 1$ is the sign of a function involving the first-order polarization coefficient. It determines whether the medium is focusing ($\alpha = -1$) or defocussing ($\alpha = +1$). Again we normalize $R(\mathbf{r})$ such that $\int_{-\infty}^{\infty} R(\mathbf{r}) d\mathbf{r} = 1$ and $R(\mathbf{0}) > 0$. In this application, $R(\mathbf{r})$ is different from the kernel $R(\mathbf{r})$ of the BEC example, due to causality. In a BEC, $R(\mathbf{r})$ is a symmetric function, where as in nonlinear optics, $R(\mathbf{r})$ is a one-sided response. The one-sided kernel introduces Raman effects which cause gain or loss [8]. In the applications we consider, we neglect Raman effects and assume a short-time response thus approximating $R(\mathbf{r})$ to be symmetric. If the medium has an instantaneous response, $R(\mathbf{r})$ is approximated by a delta function $\delta(\mathbf{r})$, again resulting in Eq. (2) [3].

Equation (1) is a Hamiltonian system [11] with Hamiltonian functional (energy)

$$H(\psi, \psi^*) = \int_{-\infty}^{\infty} \left(\frac{1}{2} |\nabla \psi|^2 + \frac{\alpha}{2} |\psi|^2 \int_{-\infty}^{\infty} R(\mathbf{r}-\mathbf{r}') |\psi|^2 d\mathbf{r}' \right) d\mathbf{r}. \quad (3)$$

Along with H , two other quantities are conserved, the L_2 norm L and the momentum P

$$\begin{aligned} L &= \int_{-\infty}^{\infty} |\psi(\mathbf{r})|^2 d\mathbf{r}, \\ P &= \frac{i}{2} \int_{-\infty}^{\infty} \left(\psi(\mathbf{r}) \nabla \psi^*(\mathbf{r}) - \psi^*(\mathbf{r}) \nabla \psi(\mathbf{r}) \right) d\mathbf{r}. \end{aligned} \quad (4)$$

In what follows, we discuss the linear and nonlinear stability of plane wave solutions of Eq. (1) and show that the nonlocal kernel $R(\mathbf{r})$ has a profound effect on the stability and behavior of these solutions. The conserved quantities are used in Arnold's method [9, 10, 11] to obtain conditions on $R(\mathbf{r})$ for nonlinear (Lyapunov) stability of plane wave solutions.

2 Review of Linear Stability for Plane Wave Solutions

Before proceeding to examine nonlinear stability, it is imperative to review the well-known results for linear stability [13, 14, 15]. In Sec. 3 we establish that the condition required for nonlinear stability is identical to the known condition for linear stability which we re-derive below for completeness. In addition, the specific examples considered for linear stability are re-visited in Sec. 4 to examine the validity of the moment expansion.

Determining if a solution ψ_e of Eq. (1) is spectrally stable requires the consideration of the evolution of an infinitesimal perturbation. This gives rise to a spectral problem $\mathcal{L}u = \lambda u$, where \mathcal{L} is a linear operator, u is the perturbation, and λ is the growth rate of that perturbation. A solution is said to be *spectrally* stable if no part of the spectrum of \mathcal{L} has positive real part. A stronger stability definition is that of *linear* stability, which states that an infinitesimal initial perturbation will not grow, or,

$$\forall \epsilon > 0 \exists \delta > 0 : \|u(\mathbf{r}, 0)\| < \delta \Rightarrow \|u(\mathbf{r}, t)\| < \epsilon, \forall t > 0.$$

where u evolves according to $u_t = \mathcal{L}u$. Linear stability requires spectral stability plus a complete set of eigenfunctions.

Equation (1) has a class of plane wave solutions of the form

$$\psi(\mathbf{r}, t) = Ae^{-i\alpha A^2 t}. \quad (5)$$

The linear stability of these plane wave solutions is examined by considering perturbed solutions

$$\psi(\mathbf{r}, t) = [A + \epsilon(u(\mathbf{r}, t) + iv(\mathbf{r}, t)) + O(\epsilon^2)]e^{-i\alpha A^2 t}, \quad (6)$$

where $0 < \epsilon \ll 1$, and u and v are real-valued functions. Neglecting terms of $O(\epsilon^2)$ and separating into real and imaginary parts we obtain,

$$\begin{aligned} u_t &= -\frac{1}{2}\nabla^2 v, \\ v_t &= \frac{1}{2}\nabla^2 u - 2\alpha A^2 \int_{-\infty}^{\infty} R(\mathbf{r} - \mathbf{r}')u(\mathbf{r}')d\mathbf{r}'. \end{aligned} \quad (7)$$

Assuming $u(\mathbf{r}, t) = u(\mathbf{r})e^{\lambda t}$, $v(\mathbf{r}, t) = v(\mathbf{r})e^{\lambda t}$ and taking the Fourier transform of Eq. (7) gives

$$\begin{pmatrix} -\lambda & \frac{1}{2}\mathbf{k}^2 \\ -\frac{1}{2}\mathbf{k}^2 - 2\alpha A^2 \hat{R}(\mathbf{k}) & -\lambda \end{pmatrix} \begin{pmatrix} \hat{u} \\ \hat{v} \end{pmatrix} = 0. \quad (8)$$

Here $\mathbf{k}^2 = k_1^2 + k_2^2 + k_3^2$ and \hat{u}, \hat{v} , and $\hat{R}(\mathbf{k})$ are the Fourier transforms of u, v , and R respectively. For the kernels we consider, $\hat{R}(\mathbf{k})$ is radially symmetric and decays as $|\mathbf{k}| \rightarrow \infty$. This system for \hat{u} and \hat{v} is a constant

coefficient linear system of equations, whose solutions can be found in terms of Fourier modes which are complete. Thus spectral stability of plane wave solutions of Eq. (1) implies linear stability. Looking for non-trivial solutions we equate the determinant of Eq. (8) to zero and obtain the growth rates

$$\lambda^2 = -\frac{1}{2}\mathbf{k}^2 \left(\frac{1}{2}\mathbf{k}^2 + 2\alpha A^2 \hat{R}(\mathbf{k}) \right). \quad (9)$$

This is a well-known result. It appears it was derived first in [13], but independently re-derived by Bang et al [14, 15]. Perturbations will grow if $\lambda^2 > 0$, or if

$$\alpha \hat{R}(\mathbf{k}) < -\frac{\mathbf{k}^2}{4A^2}. \quad (10)$$

This condition provides a convenient relationship between the Fourier transform of the nonlocal kernel and what we define to be the stability curve $\mathcal{S}_\alpha(\mathbf{k}) = -\alpha\mathbf{k}^2/4A^2$ (See Fig. 1). Along the stability curve and on $k = 0$ we have $\lambda = 0$. The stability curve separates the (\mathbf{k}, λ) plane into stable and unstable regions. For the sake of convenience, we let $k_2 = k_3 = 0$ in all examples. It is clear from the preceding discussion that this does not affect the generality of our conclusions.

2.1 Step Interaction Potential

To show the impact of nonlocality we take the interaction potential/time response to be a step function

$$R(x) = \begin{cases} 1/2\sigma & \text{if } |x| < \sigma, \\ 0 & \text{if } |x| > \sigma \end{cases} \iff \hat{R}(k) = \frac{\sin(k\sigma)}{k\sigma}. \quad (11)$$

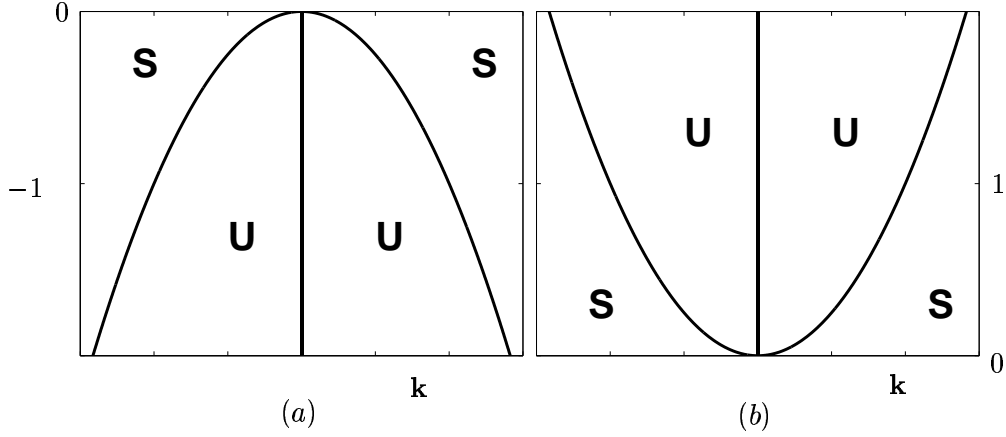


Figure 1: Stability curves (a) repulsive/defocussing ($\alpha = 1$), (b) attractive/focusing ($\alpha = -1$). For both panels, $\lambda = 0$ on the center line $\mathbf{k} = 0$.

The parameter $\sigma > 0$ (not necessarily small) acts as a measure of nonlocality. As $\sigma \rightarrow 0$, Eq. (1) approaches the local limit Eq. (2) since $R(x) \rightarrow \delta(x)$. For unstable modes, Eq. (10) requires

$$\alpha \frac{\sin(k\sigma)}{k\sigma} < -\frac{k^2}{4A^2}. \quad (12)$$

If the kernel is repulsive/defocussing ($\alpha = 1$), the local equation (2) has no unstable modes [3]. However, if values of k exist that satisfy (12), then Eq. (1) does have unstable modes. Figure 2(a1) shows the numerical evolution of a perturbed plane wave using a repulsive step potential ($\alpha = 1$) with $\sigma = 2$ and $A = 1$. Figure 2(a2) displays the excited spectral modes of the perturbation, confirming that no modes are excited. Figure 2(a3) shows the absence of a real part of the growth rate, since the stability curve $\mathcal{S}_\alpha(k)$ never intersects $\hat{R}(\mathbf{k})$, Fig. 2(a4). Figure 2(b1) displays the numerical evolution of a perturbed plane wave using a repulsive/defocussing step function kernel with $\sigma = 7$. We see that perturbations have grown significantly at time $t^* = 160$. In Fig. 2(b2) the excited modes are shown near the onset of instability. The growth rate confirms the first unstable modes excited correspond to the largest growth rate, Fig. 2(b3). The positive growth rate occurs when $\hat{R}(k) < \mathcal{S}_\alpha(k)$, see Fig. 2(b4). These examples show that the presence of the nonlocality in Eq. (1) can generate an instability that has no counterpart in the local limit.

For $\alpha = -1$ the local equation (2) has an unstable band around $k = 0$ of width $2\sqrt{2}A$ due to the standard modulational instability [3]. With $\alpha = -1$, the nonlocal equation (1) has a narrower unstable band resulting in a smaller growth rate.

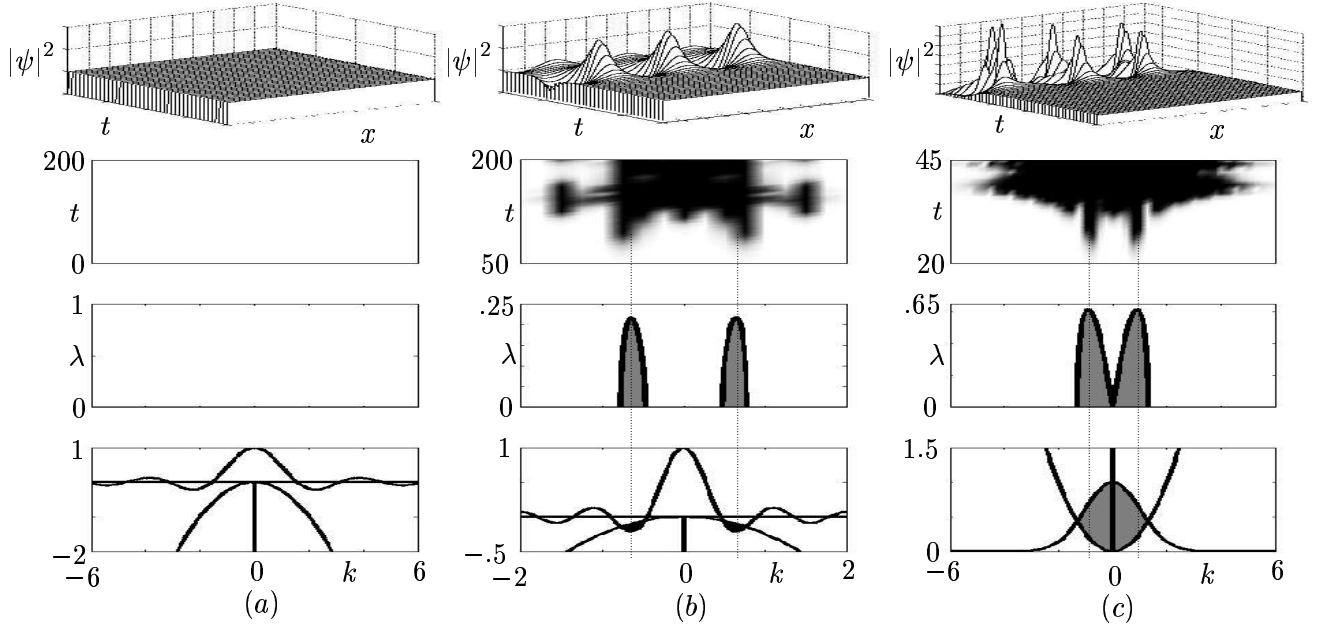


Figure 2: Perturbed plane wave ($A = 1$) evolution with : (a) a repulsive step function interaction with $\sigma = 2$, (b) a repulsive step function interaction with $\sigma = 7$, and (c) an attractive Gaussian interaction with $\sigma = 1$. In (a)-(c) dark-grey shaded areas indicate unstable modes. The top two figures (rows 1,2) show the dynamics of the solution and the growth of the perturbed Fourier modes. The bottom two figures (rows 3,4) are the analytic predictions given by Eq. (9) and Eq. (10). Notice that in (b) unstable modes are present for Eq. (1). These have no counterpart in Eq.(2).

2.2 Gaussian Interaction Potential

As a second example, consider the Gaussian potential/time response

$$R(x) = \frac{1}{\sqrt{2\pi}\sigma} e^{-x^2/2\sigma^2} \iff \hat{R}(k) = e^{-\sigma^2 k^2/2}. \quad (13)$$

Again the parameter σ acts as a measure of nonlocality, and the local limit corresponds to $\sigma \rightarrow 0$ since $R(x) \rightarrow \delta(x)$. From (10), unstable modes occur for k values when

$$\alpha e^{-k^2\sigma^2/2} < -\frac{k^2}{4A^2}. \quad (14)$$

Thus, if $\alpha = 1$ there are no unstable modes since the left-hand side of Eq. (14) is positive.

For an attractive potential/defocussing medium ($\alpha = -1$), there is a band of unstable modes around $k = 0$. Figures 2(c1) and 2(c2) show the numerical evolution of a perturbed plane wave ($A = 1$) and the excited modes, respectively, using Eq. (13) with $\sigma = 1$. Again there is agreement between the excited modes and the modes where the growth rate is maximized, Figs. 2(c3) and 2(c4). The effect of the nonlocality in this example is to narrow the band of unstable modes and reduce the growth rate.

In summary, if we consider an attractive interaction (BEC) or focusing medium (optics) (where $\alpha = -1$), Eq. (10) will be satisfied for some modes around $|\mathbf{k}| = 0$, and the plane wave solutions given by Eq. (5) are spectrally unstable. However, for a repulsive interaction (BEC) or defocussing medium (optics) (where $\alpha = +1$), plane wave solutions are *linearly* stable if for all \mathbf{k}

$$-\mathbf{k}^2/4A^2 < \hat{R}(\mathbf{k}). \quad (15)$$

3 Nonlinear Stability Analysis for Plane Wave Solutions

A more comprehensive and intuitive definition for the stability of an equilibrium solution of a conservative system is given by nonlinear (Lyapunov) stability. However, nonlinear stability is not often analytically tractable. Therefore, it is seldom considered, as opposed to the weaker concepts of spectral or linear stability. Here, we are able to prove rigorously the full nonlinear stability for plane wave solutions of Eq. (1) for a repulsive interaction potential (BEC) or defocussing medium (optics).

If we write the perturbed solution of Eq. (1) as $\psi = \psi_e + \delta\psi$ for some finite perturbation $\delta\psi$, ψ_e is nonlinearly stable if $\forall \epsilon > 0 \exists \delta > 0$ such that

$$\|\psi(\mathbf{r}, 0) - \psi_e(\mathbf{r})\| < \delta \Rightarrow \|\psi(\mathbf{r}, t) - \psi_e(\mathbf{r})\| < \epsilon, \quad \forall t > 0.$$

To prove nonlinear stability for plane wave solutions of Eq. (1) we use Arnold's method [9, 10, 11] which exploits the Hamiltonian structure and constants of motion of Eq. (1). This method consists of three key steps.

1. Construct a conserved "energy" functional V by taking a linear combination of the constants of motion, each with arbitrary coefficient. Choose the coefficients such that the first variation of V , δV , is equal to zero at the equilibrium solution

$$\delta V(\psi_e) = 0.$$

Given this condition, the equilibrium solution ψ_e is an extremum of the energy functional V .

2. Show that the second variation of V at the equilibrium solution, $\delta^2 V$, is positive definite,

$$\delta^2 V \geq 0, \quad \text{and} \quad \delta^2 V = 0 \Rightarrow \delta\psi = 0.$$

Then the equilibrium solution ψ_e is a local minimum of the energy functional V .

3. Finally, find a norm $\|\cdot\|$, and positive constants c and C such that the convexity condition

$$c\|\delta\psi\|^2 \leq V(\psi_e + \delta\psi) - V(\psi_e) \leq C\|\delta\psi\|^2$$

holds for any sufficiently small $\delta\psi$ in the function space defined by this norm.

Plane wave solutions are a special class of stationary solutions to Eq. (1). Stationary solutions of Eq. (1) are of the form $\psi_e(\mathbf{r}, t) = \phi(\mathbf{r}) e^{-i\omega t}$, where ϕ satisfies the equation

$$\frac{1}{2}\nabla^2\phi + \omega\phi - \phi \int_{-\infty}^{\infty} R(\mathbf{r}-\mathbf{r}') |\phi(\mathbf{r}')|^2 d\mathbf{r}' = 0. \quad (16)$$

For Eq. (1), we use Eq. (3) and Eq. (4) to obtain a conserved functional of the form

$$V(\psi, \psi^*, \nabla\psi, \nabla\psi^*) = \beta_1 L + \beta_2 P + \beta_3 H. \quad (17)$$

Using ψ_e , Eq. (16), and requiring $\delta V(\psi_e, \psi_e^*, \nabla\psi, \nabla\psi^*) = 0$ determines the coefficients $\beta_1 = -\omega$, $\beta_2 = 0$, and $\beta_3 = 1$. The “energy” functional which has an extremum at ψ_e is

$$V = \int_{-\infty}^{\infty} \left(\frac{1}{2} |\nabla\psi|^2 - \omega |\psi|^2 + \frac{1}{2} |\psi|^2 \int_{-\infty}^{\infty} R(\mathbf{r}-\mathbf{r}') |\psi|^2 d\mathbf{r}' \right) d\mathbf{r}.$$

Expanding V about the equilibrium solution we have $V(\psi_e + \delta\psi) = V(\psi_e) + \delta V(\psi_e, \psi_e^*) + \delta^2 V(\psi_e, \psi_e^*) + \dots$. The second variation of V , $\delta^2 V(\psi, \psi^*)$ is a quadratic form in $\delta\psi$. We calculate $\delta^2 V$ from $\Delta V = V(\psi_e + \delta\psi) - V(\psi_e) = V((\phi + u + iv) e^{-i\omega t}) - V(\phi e^{-i\omega t})$, where we have decomposed the perturbation into its real and imaginary parts $\delta\psi = u + iv$. Letting $\phi = A$ and $\omega = -A^2$ for plane waves, we find

$$\Delta V = \Delta K + \Delta T, \quad (18)$$

with

$$\Delta K = \int_{-\infty}^{\infty} \frac{1}{2} \left((\nabla u(\mathbf{r}))^2 + (\nabla v(\mathbf{r}))^2 \right) d\mathbf{r}, \quad (19)$$

$$\begin{aligned} \Delta T = & \int_{-\infty}^{\infty} \left[2A(u^2(\mathbf{r}) + v^2(\mathbf{r}) + Au(\mathbf{r})) \int_{-\infty}^{\infty} R(\mathbf{r}-\mathbf{r}') u(\mathbf{r}') d\mathbf{r}' \right. \\ & \left. + \frac{1}{2} (u^2(\mathbf{r}) + v^2(\mathbf{r})) \int_{-\infty}^{\infty} R(\mathbf{r}-\mathbf{r}') (u^2(\mathbf{r}') + v^2(\mathbf{r}')) d\mathbf{r}' \right] d\mathbf{r}. \end{aligned} \quad (20)$$

$\Delta V(u, v, \nabla u, \nabla v)$ depends on the kernel $R(\mathbf{r})$, the real-valued functions u, v , and their derivatives $\nabla u, \nabla v$. The conditions for which $\Delta K + \Delta T$ is strictly positive can be found by observing from Eq. (19),

$$\begin{aligned}
\Delta K &= \int_{-\infty}^{\infty} \frac{1}{2} \left((\nabla u(\mathbf{r}))^2 + (\nabla v(\mathbf{r}))^2 \right) d\mathbf{r} \\
&\geq \int_{-\infty}^{\infty} \frac{1}{2} (\nabla u(\mathbf{r}))^2 d\mathbf{r} \\
&= \int_{-\infty}^{\infty} \frac{1}{2} \mathbf{k}^2 |\hat{u}(\mathbf{k})|^2 d\mathbf{k} \\
&= \Delta K',
\end{aligned} \tag{21}$$

which defines $\Delta K'$. Note that we have used Parseval's equality [17] to obtain Eq. (21).

From Eq. (20) ΔT depends only on u and v . Taking the variation of ΔT with respect to u and v we find ΔT has an isolated extremum at the point $(u, v) = (-A, 0)$ and a circle of extrema at $\mathcal{N} : (u + A)^2 + v^2 = A^2$ (thick circle in Fig. 3). At the point $(-A, 0)$, $\Delta T = A^4/2 > 0$ and thus ΔT has a local maximum. Along the circle \mathcal{N} , $\Delta T = 0$. \mathcal{N} is a neutral stability curve for the system. The effect of a perturbation along \mathcal{N} is given by

$$|\psi_e + \delta\psi|^2 = |A + u + iv|^2 = (A + u)^2 + v^2 = A^2 = |\psi_e|^2.$$

Thus, along \mathcal{N} , ψ_e is perturbed only in phase. Since Eq. (1) is phase-invariant, perturbations along \mathcal{N} may be ignored. To examine how ΔT behaves under perturbations away from \mathcal{N} , we parameterize Eq. (20) by

$$\begin{aligned}
u_p(\epsilon, \theta) &= A(1 + \epsilon)(\cos \theta - 1), \\
v_p(\epsilon, \theta) &= A(1 + \epsilon)\sin \theta,
\end{aligned}$$

for $|\epsilon| \ll 1$ and $\theta \in [0, 2\pi]$ (note as $\epsilon \rightarrow 0$ the perturbed curve (thin circles in Fig. 3) approaches \mathcal{N}). With this parameterization and $u_p^2 + v_p^2 = 2A^2(1 + \epsilon)^2(1 - \cos \theta)$ we have

$$\Delta T = 2\epsilon^2 A^2 \int_{-\infty}^{\infty} \left(u_p(\mathbf{r}) \int_{-\infty}^{\infty} R(\mathbf{r}-\mathbf{r}') u_p(\mathbf{r}') d\mathbf{r}' \right) d\mathbf{r}. \tag{22}$$

Using Parseval's equality (* denotes convolution),

$$\langle u(\mathbf{r}) | R(\mathbf{r}) * u(\mathbf{r}) \rangle = \langle \hat{u}(\mathbf{k}) | \hat{R}(\mathbf{k}) \hat{u}(\mathbf{k}) \rangle,$$

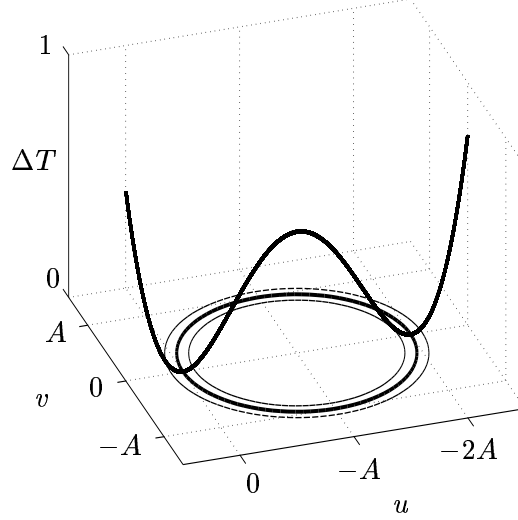


Figure 3: Phase-invariant neutral stability curve \mathcal{N} (thick). Perturbations of this curve (thin). A slice of ΔT ($v = 0$) is shown for delta function kernel: $R(\mathbf{r}) = \delta(\mathbf{r})$. Note that $\Delta T = 0$ for $(u, v) \in \mathcal{N}$, and is positive off this curve.

gives

$$\Delta T = 2\epsilon^2 A^2 \int_{-\infty}^{\infty} \hat{R}(\mathbf{k}) |\hat{u}_p(\mathbf{k})|^2 d\mathbf{k}. \quad (23)$$

To describe $\delta^2 V$ away from \mathcal{N} , we have expressed ΔK and ΔT in terms of spectral integrals. Thus on circles away from \mathcal{N} we have

$$\begin{aligned} \Delta V &= \Delta K + \Delta T \\ &\geq \Delta K' + \Delta T \\ &= \int_{-\infty}^{\infty} \frac{1}{2} \mathbf{k}^2 |\hat{u}_p(\mathbf{k})|^2 d\mathbf{k} + 2\epsilon^2 A^2 \int_{-\infty}^{\infty} \hat{R}(\mathbf{k}) |\hat{u}_p(\mathbf{k})|^2 d\mathbf{k} \\ &\geq \epsilon^2 \int_{-\infty}^{\infty} \frac{1}{2} \mathbf{k}^2 |\hat{u}_p(\mathbf{k})|^2 d\mathbf{k} + 2\epsilon^2 A^2 \int_{-\infty}^{\infty} \hat{R}(\mathbf{k}) |\hat{u}_p(\mathbf{k})|^2 d\mathbf{k} \\ &= 2\epsilon^2 A^2 \int_{-\infty}^{\infty} \left(\frac{\mathbf{k}^2}{4A^2} + \hat{R}(\mathbf{k}) \right) |\hat{u}_p(\mathbf{k})|^2 d\mathbf{k}. \end{aligned} \quad (24)$$

Thus if (15) is satisfied, the second variation of V , $\delta^2 V$ is strictly positive.

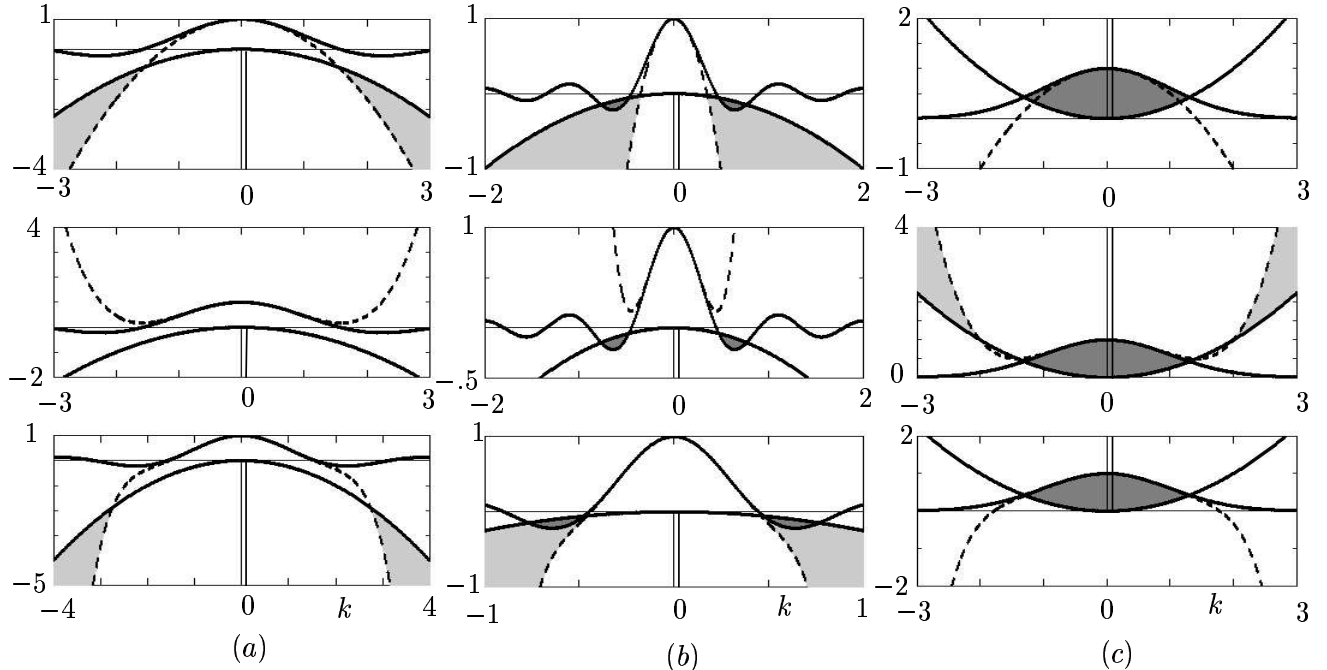


Figure 4: The 1- (top), 2- (middle), and 3- (bottom) term expansions for: (a) a repulsive/defocussing step kernel with $\sigma = 2$, $A = 1$, (b) a repulsive/defocussing step kernel with $\sigma = 7$, $A = 1$, and (c) an attractive/focusing Gaussian kernel with $\sigma = 1$, $A = 1$. Dark-gray shaded regions indicate unstable modes present in the fully nonlocal equation (1) whereas light-gray shaded regions indicate unstable modes present in the moment approximation (25). The validity of the moment expansion breaks down in the light-gray regions corresponding to high-wavenumber instabilities (characteristic of an ill-posed equation).

From Eq. (19) and Eq. (20), ΔV is a quadratic form in u , v , ∇u , and ∇v allowing the convexity condition to be satisfied using the L_2 norm:

$$\Delta V(u, v, \nabla u, \nabla v) < C \int_{-\infty}^{\infty} (u^2 + v^2) dx.$$

Thus we have found $\delta V = 0$ for plane wave solutions Eq. (5). For suitable perturbations, the second variation of V , $\delta^2 V$, is positive definite if Eq. (15) is satisfied. These conditions prove that plane wave solutions of Eq. (1) satisfying Eq. (15) are *nonlinearly stable* in the L_2 norm.

4 Stability of Plane-Wave Solutions of the N -Moment Expansion

An often-used approximation [14, 16] of Eq. (1) is

$$i\psi_t = -\frac{1}{2}\nabla^2\psi + \alpha \sum_{n=0}^N \gamma_{2n}\psi \nabla^{2n} |\psi|^2, \quad (25)$$

where $\gamma_{2n} = 1/(2n)! \int_{-\infty}^{\infty} R(\mathbf{s}) \mathbf{s}^{2n} d\mathbf{s}$. This is obtained using a change of variables $\mathbf{z} = \mathbf{r} - \mathbf{r}'$ followed by a truncated Taylor expansion of $|\psi|^2$ around $\mathbf{r}' = 0$ in Eq. (1). The question is whether this approximation changes the stability properties of the nonlocal problem.

Repeating the linear stability calculations for Eq. (25) in exactly the same way as for Eq. (1) we obtain the growth rate

$$\lambda^2 = -\frac{1}{2}\mathbf{k}^2 \left(\frac{1}{2}\mathbf{k}^2 + 2\alpha A^2 \sum_{n=0}^N (-1)^n \gamma_{2n} \mathbf{k}^{2n} \right). \quad (26)$$

This result is equivalent to replacing $\hat{R}(\mathbf{k})$ with the $2N$ -th order Taylor expansion $\hat{R}_N(\mathbf{k})$ in Eq. (9). For unstable modes

$$\alpha \sum_{n=0}^N (-1)^n \gamma_{2n} \mathbf{k}^{2n} < -\frac{\mathbf{k}^2}{4A^2}. \quad (27)$$

The moment expansion for the integral in Eq. (1) gives a stability relation involving the same stability curve \mathcal{S}_α , and $\hat{R}_N(\mathbf{k})$. The validity of the approximation Eq. (25) to Eq. (1) can be deduced from Eq. (27). In particular, the approximation can lead to the introduction of two unphysical results:

- Since $\hat{R}_N(\mathbf{k}) \rightarrow \pm\infty$ as $|\mathbf{k}| \rightarrow \pm\infty$, the moment expansion can give rise to non-physical high-frequency instabilities which are characteristic of a mathematically ill-posed problem [17].
- The approximation can predict (nonlinear) stability when the fully nonlocal solutions are unstable.

4.1 Repulsive/Defocussing Step Kernel

If $R(x)$ is given by Eq. (11), $\sigma^{2n}/(2n+1)! = \gamma_{2n}$. Figure 3(a1) displays the stability curve \mathcal{S}_α , $\hat{R}(k)$ (solid), and the one-term expansion $\hat{R}_1(k)$ (dashed). Here $\sigma = 2$ and $A = 1$. Since the curvature of \hat{R}_1 exceeds that of the stability curve, non-physical high-frequency modes are excited resulting in an ill-posed approximation. In Fig. 3(a2), the two-term moment expansion $\hat{R}_2(k)$ approaches $+\infty$ as $|k| \rightarrow \infty$. Thus no non-physical modes are excited and the plane-wave solution is nonlinearly stable. Figure 3(a3) illustrates the case of a three-term moment expansion. This shows that for any

odd integer greater than one, the moment expansion is ill-posed, independent of the parameters. In Fig. 3b we use a repulsive/defocussing kernel with $\sigma = 7$. Figures 3(b1) and 3(b3) display ill-posed models using the one-term and three-term moment expansion, respectively. In Fig. 3(b2) we see that the two-term moment expansion does not give rise to non-physical modes. However, it fails to predict physical unstable modes present in the fully nonlocal equation. This approximation represents a nonlinearly stable plane wave solution where the plane wave is spectrally unstable for the nonlocal equation.

4.2 Attractive/Focusing Gaussian Kernel

If $R(x)$ is given by Eq. (13), $\sigma^{2n}/(2n)!! = \gamma_{2n}$, where $!!$ is the standard double factorial [18, pages 544-545]. Figures 3(c1) and 3(c3) show the one-term and three-term moment expansions, respectively. As N (odd integer) increases, the moment expansion better represents the fully nonlocal equation. Figure 3(c2) illustrates the case $N = 2$. In this case non-physical high-frequency modes are excited, and the moment expansion leads to an ill-posed approximation of the nonlocal equation.

In summary, if Eq. (1) is approximated by the moment expansion Eq. (25), the number of terms kept in the approximation is crucial to avoid an ill-posed approximation of Eq. (1). For a repulsive/defocussing ($\alpha = +1$) kernel, a 1-term expansion is ill-posed if $\gamma_2 > 1/(4A^2)$. An even-term expansion does not give rise to high-frequency instabilities, but it may fail to predict instabilities present in the nonlocal equation. An odd-term expansion with more than one term leads to an ill-posed approximation independent of the value of the parameters. For an attractive/focusing kernel ($\alpha = -1$), an odd term expansion approximates the governing nonlocal equation well. The more terms kept in the expansion, the better the representation of the unstable band around $|\mathbf{k}| = 0$. An even-term expansion gives rise to an ill-posed model.

5 Conclusions

Nonlocality in the governing evolution equation (1) has profound effects. For a repulsive/defocussing kernel, ($\alpha = 1$), unstable side bands that do not have counterparts in the local case can be generated. For an attractive/focusing interaction there is always an unstable symmetric band around $|\mathbf{k}| = 0$. The nonlocality reduces the width of that band and the resulting growth rate. The linear stability results for Eq. (2) are consistent with previous findings of Bang et al [14, 15]. From the stability calculations of plane wave solutions of Eq. (1), it is clear the nonlocal perturbation gives rise to behavior that is significantly different than that of the local model (2). The behavior is analyzed using the stability curves \mathcal{S}_α and the Fourier transform of the interaction potential in Eq. (10).

A more intuitive definition for the stability of an equilibrium solution to a conservative system is given by nonlinear stability, which is often difficult to prove. Remarkably, if the Fourier transform

of the repulsive/defocussing ($\alpha = 1$) kernel is greater than the stability curve $S_\alpha(\mathbf{k})$ for all \mathbf{k} , plane wave solutions to Eq. (1) are *nonlinearly* stable.

Approximating Eq. (1) by Eq. (25) can give rise to non-physical high-frequency instabilities, defining an ill-posed approximation. It can also predict stability when the plane wave solutions to Eq. (1) are unstable. The effectiveness of the moment expansion is easily analyzed using the same stability curves S_α and the Taylor expansion of the Fourier transform of the nonlocal kernel in Eq. (27).

Acknowledgements

This material is based upon work supported by the National Science Foundation under grant Nos. DMS-VIGRE 0354131, DMS-0139093, and DMS-0092682. We wish to acknowledge useful discussions with Jared C. Bronski and Harvey Segur.

References

- [1] E.P. Gross, *Nuovo Cimento* 20, 454, 1960.
- [2] L.P. Pitaevskii, *Sov. Phys. JETP*, 13:451, 1961.
- [3] G.P. Agrawal, *Nonlinear Fiber Optics*, Academic Press, New York, 1989.
- [4] G. Baym, *Lectures on Quantum Mechanics*, Addison-Wesley, Redwood City CA, 1990.
- [5] G.B. Whitham, *Linear and Nonlinear Waves*, Wiley, New York, 1974.
- [6] E. H. Lieb and R. Seiringer, *Phys. Rev. Lett.* 88:170409, 2002.
- [7] B. Deconinck and J. N. Kutz, *Phys. Lett. A* 319:97-103, 2003.
- [8] R.W. Hellwarth, *Progress in Quantum Electronics* 5:1-68, 1977.
- [9] V.I. Arnold, *Doklady Mat Nauk.* 162(5):773-777, 1965.
- [10] V.I. Arnold, *Am. Math. Soc. Transl.* 19:267-269, 1965.
- [11] G.E. Swaters, *Introduction to Hamiltonian Fluid Dynamics and Stability Theory*, Chapman and Hall, London, 2000.
- [12] D. D. Holm, J. E. Marsden, T. Ratiu and A. Weinstein, *Physics Reports* 64:226, 1984.
- [13] J. C. Bronski, *Aspects of Randomness in Nonlinear Wave Propagation*, Ph.D thesis, Princeton University, 1994.

- [14] W. Krolikowski, O. Bang, J.J. Rasmussen and J. Wyller, Phys. Rev. E 64:016612, 2001.
- [15] J. Wyller, W. Krolikowski, O. Bang and J. J. Rasmussen, Phys. Rev. E 66:066615, 2002.
- [16] S.T. Turitsyn, Teor. Mat. Fiz. 64:226, 1985.
- [17] R.B. Guenther and J.W. Lee, *Partial Differential Equations of Mathematical Physics and Integral Equations*, Dover Publications Inc., New York, 1988.
- [18] G. Arfken, *Mathematical Methods for Physicists*, Academic Press, Orlando, Fl., 1985.